

## ORIGINAL ARTICLE

# Strain-induced $^{13}\text{C}$ chemical shift change of natural rubber

Masashi Kitamura<sup>1</sup>, Yoshiaki Hata<sup>2</sup>, Hiroshi Yasuoka<sup>2</sup>, Takuzo Kurotsu<sup>1</sup> and Atsushi Asano<sup>1</sup>

We investigated the effect of deformation of natural rubbers (NR) resulting from the high centrifugal pressure of fast magic-angle spinning (MAS) on  $^{13}\text{C}$  NMR spectra. The solid state  $^{13}\text{C}$  MAS NMR spectrum with high-power  $^1\text{H}$  dipolar decoupling (DD) of NR presents liquid-like, very narrow signals (full width at half height, FWHH, is less than 10 Hz). However, the static state  $^{13}\text{C}$  DD NMR spectrum of the NR after MAS presented broad and apparently anisotropic peaks for the restricted elongated (doughnut-shaped) NR (FWHH is approximately 280 Hz), although the static  $^{13}\text{C}$  NMR spectrum before MAS exhibited an isotropic and relatively narrow peak (FWHH is 150 Hz). Furthermore, the  $^{13}\text{C}$  DD NMR peaks of the maximum elongated NR in a rotor apparently became a doublet. The static  $^{13}\text{C}$  DD NMR spectrum of a strip cut from the maximum elongated NR showed an angle dependence to the static magnetic field, and the dependence was explained from the molecular orientation. The angle-dependent  $^{13}\text{C}$  NMR spectra of a strip cut from the doughnut-shaped NR differed from those of the maximum elongated NR. The magnetization measured using a SQUID (superconducting quantum interference device) indicated that the magnetic susceptibility of the strip cut from the doughnut-shaped NR was different from the maximum elongated (rolled) NR. The difference in the angle dependence of the  $^{13}\text{C}$  DD NMR spectra was therefore attributed to not only the molecular orientation but also the difference in magnetic susceptibility caused by the  $\pi$  electron interaction with the static magnetic field.

*Polymer Journal* (2012) 44, 778–785; doi:10.1038/pj.2012.120; published online 20 June 2012

**Keywords:** centrifugal pressure;  $^{13}\text{C}$  NMR chemical shift; deformation; magnetic susceptibility; natural rubber

## INTRODUCTION

Recently, investigations of rubbers and elastomers, especially the structural study of the cross-linking region and the improvement of physical properties by adding fillers for a natural rubber (NR), have been attracting considerable attention because rubbers and elastomers are one of essential materials for basics in a high-technology industry. Furthermore, a rise in the public interest in ecology has been widely encouraging the use of eco-friendly materials, such as NR, because they are produced from natural resources.

Nuclear magnetic resonance (NMR) is an efficient tool for investigating the structure and morphology of polymers at the molecular level. Solid state NMR is especially useful for elucidating the molecular structure of rubbers because vulcanized rubbers do not dissolve in any solvents. Kawahara *et al.*<sup>1</sup> have revealed the detailed structure of the cross-linking region in NR using solid state  $^{13}\text{C}$  NMR with a novel field gradient technique under fast magic-angle spinning (MAS) conditions. More recently, we have reported on the impact of the MAS on the solid state  $^1\text{H}$  NMR spectra of rubbers.<sup>2</sup> Styrene-butadiene rubber (SBR) in a SBR/Si composite is deformed during MAS, and its molecular motion was severely affected by fast MAS rates. The MAS technique is necessary for reducing the weak homo and hetero dipolar interactions of rubbers and elastomers to obtain

high-resolution solid state  $^1\text{H}$  and  $^{13}\text{C}$  NMR spectra. High-resolution spectra enable us to analyze the precise structure of rubbers. However, the centrifugal pressure resulting from MAS is large enough to deform rubbers, and it induces structural changes in the rubbers. Kawamura *et al.*<sup>3</sup> have previously demonstrated that a fast MAS results in structural changes of soft membrane proteins. We have also revealed that the temperature-dependent  $^1\text{H}$  spin-lattice relaxation time ( $T_1$ ) curve for SBR changes depending on the interaction strength between the SBR and the Si filler.<sup>2</sup> Furthermore, Nishiyama *et al.*<sup>4</sup> and Fry *et al.*<sup>5</sup> have reported that very-fast MAS influences the  $^1\text{H}$  and  $^{13}\text{C}$   $T_1$  values. Therefore, examining the effects of MAS on the structure of rubbers and the NMR parameters is an attractive idea.

In this paper, we report on the static and solid state  $^{13}\text{C}$  NMR spectra of a non-vulcanized natural rubber (NR) that was deformed during MAS. Kimura *et al.*<sup>6,7</sup> have reported that the stretching of vulcanized NR causes the molecular orientation in the static  $^{13}\text{C}$  NMR spectra, and the  $^{13}\text{C}$  chemical shift depends on the angle between the stretching direction and the static magnetic field. The maximum elongated NR examined using MAS presented a similar anisotropic  $^{13}\text{C}$  NMR spectrum to that observed by Kimura *et al.*<sup>6</sup> Furthermore, the angle-dependent  $^{13}\text{C}$  NMR spectra obtained from a strip cut from the maximum elongated NR also presented the same

<sup>1</sup>Department of Applied Chemistry, National Defense Academy, Yokosuka, Kanagawa, Japan and <sup>2</sup>Department of Applied Physics, National Defense Academy, Yokosuka, Kanagawa, Japan

Correspondence: Dr A Asano, Department of Applied Chemistry, National Defense Academy, Hashirimizu 1-10-20, Yokosuka, Kanagawa 239-8686, Japan.

E-mail: asanoa@nda.ac.jp

Received 30 January 2012; revised 30 April 2012; accepted 2 May 2012; published online 20 June 2012

results as those observed by Kimura *et al.*<sup>6</sup> Although similar anisotropic  $^{13}\text{C}$  NMR spectra were observed from the elongation restricted (doughnut-shaped) NR, the observed angle dependence of the  $^{13}\text{C}$  chemical shift value from the doughnut-shaped NR presents an inverse relationship to that observed by Kimura *et al.*,<sup>6</sup> however, our experimental conditions were not the same as theirs.

To investigate and understand the origin of the anisotropic  $^{13}\text{C}$  NMR spectra for a deformed NR, we first reconsidered the growth of the crystalline phase because it has been suggested that strain induces crystallization for NR (Please refer to references 1–7 listed in the current ref. 6). Second, we confirmed whether the molecular orientation occurred for the maximum extended NR thin film using angle (position)-dependent  $^{13}\text{C}$  NMR measurements. Third, we investigated the angle-dependent  $^{13}\text{C}$  NMR spectra for the restricted elongation NR. Finally, we discussed the magnetic susceptibility difference depending on the elongation ratio of NR during MAS.

## EXPERIMENTAL PROCEDURES

### Samples

The natural rubber (NR, *Hevea brasiliensis*) used in this study was RSS1 grade (Ribbed Smoked Sheet grade 1) and was obtained from the Toyota Tsusho Corporation (Nagoya, Japan) through the Advanced Elastomer research group of the Society of Rubber Industry, Japan. We used the NR as received without further purification and vulcanization, with the exception of an annealing process at 333 K in a thermostat for 1 day to melt and remove the micro-crystalline phase.

The sample preparation for the NMR measurements is illustrated in Figure 1. We controlled the NR elongation ratio during MAS using Teflon spacers of different lengths, as shown in Figure 1. The NR was deformed in a sample rotor with a MAS rate of 9 kHz at 333 K for 1 day. Each NR sample was

weighed to the same weight of 32 mg. The various lengths of the NR towards the rotor height were prepared from 3.4 mm to approximately 20 mm with 0.1 mm portions of length. Figure 1a shows an NR with a 3.4 mm length and 1.1 mm thickness (a doughnut shape), and both (b) and (c) are approximately 20 mm long and 0.2 mm thick. To observe the angle (position)-dependent  $^{13}\text{C}$  NMR spectra against the static field, the NR was cut into a strip (rectangular thin film or rectangular solid small piece) and placed into the central inner wall of a sample rotor, as shown in Figure 1d and e.

### Nuclear magnetic resonance measurements

Solid state  $^{13}\text{C}$  NMR spectra were measured using a Varian NMR systems 400WB spectrometer (Agilent Technologies, Santa Clara, CA, USA) operating at 100.57 MHz for  $^{13}\text{C}$  and 399.94 MHz for  $^1\text{H}$  at 303 K. The strength of the  $^1\text{H}$  dipolar decoupling was 48 kHz, and the  $90^\circ$  pulse length of  $^{13}\text{C}$  was 3.2  $\mu\text{s}$ . The MAS speed for a 6.0-mm $\phi$  rotor was 9 kHz for measuring the  $^{13}\text{C}$  DDMAS NMR spectra. The repetition delay was 5 s, which was five times longer than the  $^{13}\text{C}$   $T_1$ . A cross-polarization (CP) experiment was also performed to reveal the crystalline phase. The  $^{13}\text{C}$  chemical shift values were measured relative to tetramethylsilane using the methine carbon signal at 29.47 p.p.m. for solid adamantane as an external standard.

The angle (position)-dependent static state  $^{13}\text{C}$  NMR spectra were observed from  $0^\circ$  to  $315^\circ$  at an increment of  $45^\circ$ . The angle of  $0^\circ$  was defined when the cut NR strip in the rotor is positioned at the bottom, as shown in Figure 1a. Because we used a general MAS probe, the defined angle differs from the actual angle that is determined between the static magnetic field and the position of sample.

The shimming is very important for detecting the angle-dependent  $^{13}\text{C}$  NMR spectra without influence from the inhomogeneity of the applied magnetic field. The resolution of the static  $^{13}\text{C}$  NMR spectra was determined by comparing the half widths between the adamantane and NR peaks. The detailed discussion is presented later.

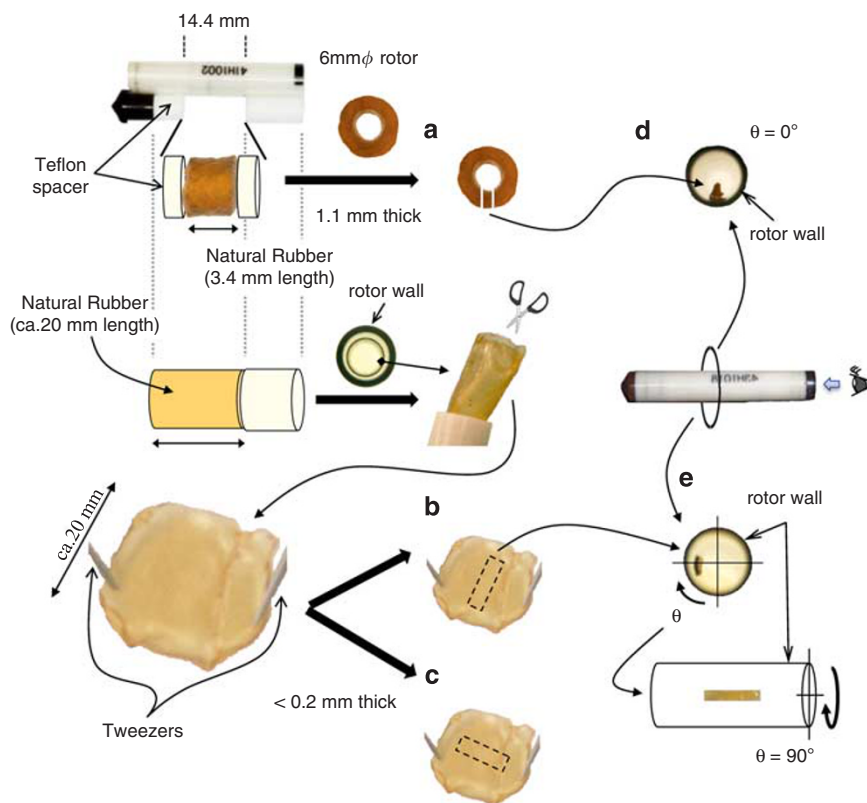


**Figure 1** Sample preparation for the expansion of NR by MAS and for measuring the angle (position)-dependent static  $^{13}\text{C}$  NMR spectra. The left-hand side is the preparation of NR with various elongation ratios. The right-hand side illustrates setting the cut strip into the rotor and the definition of angle and position. (a) a doughnut-shaped NR, (b) and (c) very thin film of the maximum extended NR, (d) and (e) definition of angle and setting of an NR strip.

### Magnetic susceptibility measurements

The magnetization,  $M$  ( $\text{A m}^2 \text{kg}^{-1}$ ), of the sample at 300 K was measured using a commercial SQUID (superconducting quantum interference device) magnetometer, Quantum Design MPMS-XL5 (Quantum Design, San Diego, CA, USA). The magnetic field strength,  $H$ , was swept from 0 to  $4 \times 10^6 \text{ A m}^{-1}$ . The mass magnetic susceptibility,  $\chi_m$  ( $\text{m}^3 \text{kg}^{-1}$ ), was calculated from the slope of the  $M$  against  $H$  plots.

### Wide-angle X-ray diffraction (WAXD)

WAXD patterns were collected using a MAC Science M21X diffractometer with  $\text{Cu K}\alpha$  radiation of  $\lambda = 0.154 \text{ nm}$  at 293 K.

## RESULTS AND DISCUSSION

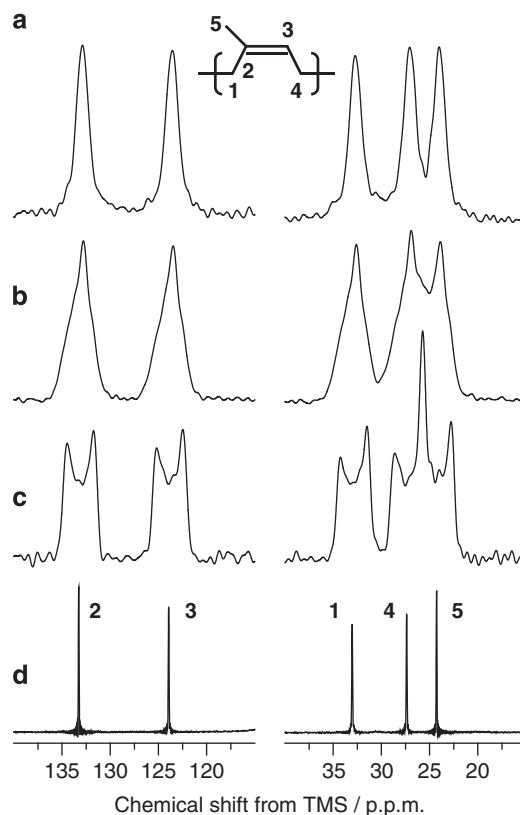
### $^{13}\text{C}$ NMR spectra of NR

Figure 2 presents the solid state  $^{13}\text{C}$  NMR spectra of NR collected with and without MAS. The  $^{13}\text{C}$  DDMAS NMR spectrum of NR shows that each of the five peaks is liquid-like and very narrow, as shown in (d). Even without the use of MAS, the static  $^{13}\text{C}$  NMR spectrum (a) of pristine NR with dipolar decoupling is significantly narrower than that of typical glassy polymers. All five peaks present an isotropic line shape. This observation results from the molecular motion of NR at 303 K, which is sufficiently fast to reduce and weaken the strong  $^1\text{H}$ - $^{13}\text{C}$  dipolar interaction in a solid; the glass transition temperature ( $T_g$ ) of NR is approximately 200 K. Interestingly, the static  $^{13}\text{C}$  NMR spectra after MAS at 9 kHz do not present an isotropic line shape, but are anisotropic peaks, as in (b) and (c). The difference between (b) and (c) is the thickness and elongation ratio of NR following MAS. The elongation of NR for (b) is restricted at 3.4 mm length, and then the shape becomes a doughnut-like cylinder with a thickness of 1.1 mm, as shown in Figure 1a. The NR of (c) becomes rolled into a very thin film with a thickness of less than 0.2 mm. The length of the NR is approximately 20 mm, and the maximum value is obtained when the NR is elongated by MAS.

The  $^{13}\text{C}$  chemical shifts of the peak top of the doughnut-shaped NR (b) are the same as those of pristine NR (a). However, the  $^{13}\text{C}$  NMR spectrum of the NR film presents a doublet-like peak. The separation of the doublet top is 2.7 p.p.m. (276 Hz), and the two peaks are identically separated from the isotropic chemical shift value in (d). The apparent two peaks also appeared in (b) as a shoulder peak that is overlapped on the center peak. Kimura *et al.*<sup>6</sup> have observed a similar spectral pattern for a stretched, vulcanized NR band with an extension ratio of 2. Those authors concluded that the doublet peak results from the summation of each peak, which is observed in the angle-dependent  $^{13}\text{C}$  NMR spectra between the stretching and the static magnetic field directions.

Because it has been suggested that strain induces crystallization in NR, we firstly observed the WAXD patterns of the maximum elongated NR to confirm the existence of a crystalline phase. Figure 3 presents the static  $^{13}\text{C}$  NMR spectra of three types of NR (A) and the WAXD patterns (B). Figure 3Aa shows the methine carbon for the maximum extended NR thin film, and 3Ab shows the methine carbon without elongation after annealing at 333 K for 1 day. Figure 3Ac is obtained from the as-received pristine NR before annealing, and 3Ad is obtained from the as-received pristine NR with the CP enhancement.

Figure 3Ac shows an isotropic, symmetrical peak and the NR after annealing (b), except for the  $^{13}\text{C}$  chemical shift value. The chemical shift value of NR before annealing is 123.0 p.p.m.; after annealing, the chemical shift value is 123.6 p.p.m. Furthermore, the linewidth becomes broader after annealing. Figure 3Ad is the  $^{13}\text{C}$  CP NMR



**Figure 2** Solid state static  $^{13}\text{C}$  NMR (a–c) and  $^{13}\text{C}$  DDMAS NMR spectra (d) of NR. Spectrum (a) is obtained before MAS, and both spectra of (b) and (c) are observed after MAS at 9 kHz for 1 day at 333 K. The sample (b) is not elongated, but its shape became doughnut-like owing to high inner pressure caused by MAS. The elongation of (c) is the maximum, approximately 20 mm. The same  $^{13}\text{C}$  DDMAS NMR spectra as (d) were observed for both samples (b) and (c).

spectrum without MAS of the same sample of (c). The  $^{13}\text{C}$  CP NMR spectrum clearly shows the additional peak at 124.0 p.p.m.

Lin *et al.*<sup>8</sup> observed two similar peaks for a vulcanized NR in a  $^{13}\text{C}$  CPMAS NMR spectrum. Those authors concluded that the lower-field peak arises from the crystalline phase from the difference between the  $^{13}\text{C}$  CPMAS and DDMAS NMR spectra. The lower-field peak is only detected in the  $^{13}\text{C}$  CPMAS NMR spectrum because the CP experiment significantly enhances the less mobile signal. Moreover, a conformation of the bond between methylene carbons in amorphous phase will give rise to the  $\gamma$  effect on  $^{13}\text{C}$  chemical shift rather than that in the crystalline phase; therefore, the  $^{13}\text{C}$  chemical shift of the amorphous phase is shifted toward a higher field than that of the crystalline phase. Therefore, our current peak at 124.0 p.p.m. that was only observed in the CP experiment is also attributed to the crystalline phase.

To confirm the presence of the crystalline phase, we examined the WAXD patterns for three samples. Figure 3Bc indicates that the as-received pristine NR presents several sharp peaks, which are related to the crystalline phase. In contrast, the WAXD pattern of the annealed NR does not present such a sharp peak, but only a broad peak at approximately  $2\theta = 19.3^\circ$  that is attributed to an amorphous phase (3Bb). Therefore, the peak at 124.0 p.p.m. is assigned to the crystalline phase. The halo peak at  $2\theta = 19.3^\circ$  in the WAXD pattern for the NR before annealing indicates that the peak at 123.0 p.p.m. is ascribed to the amorphous phase.

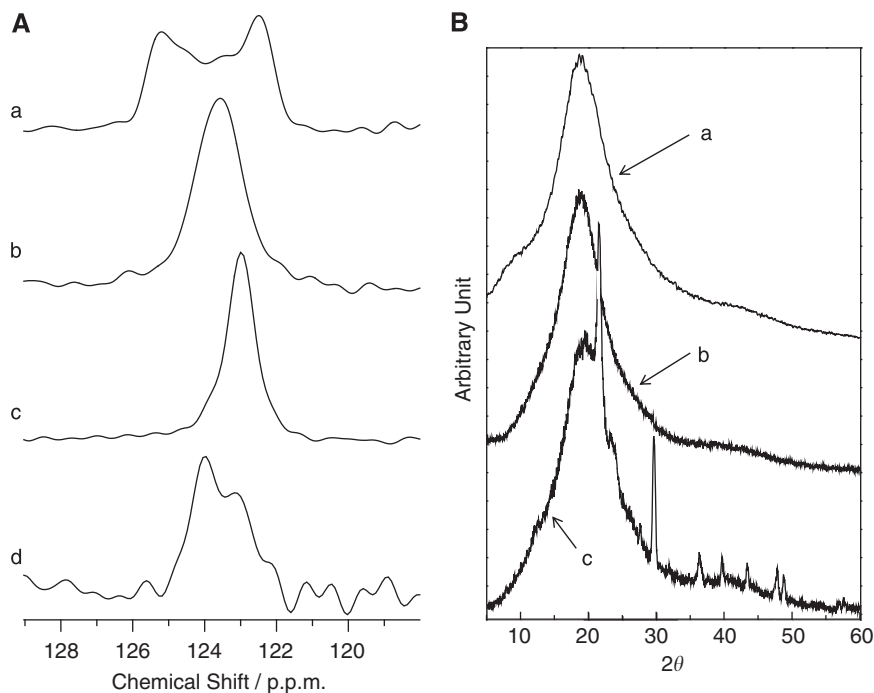


**Figure 3** Solid state static  $^{13}\text{C}$  NMR (A) and the WAXD patterns (B). Spectra A-(a) and A-(b) are the same spectra of the methine carbon region as (c) and (a), respectively. A-(a) is obtained from the maximum elongated NR and A-(b) after annealing. Spectrum A-(c) is obtained from the as-received NR before annealing. Spectrum A-(d) is the static  $^{13}\text{C}$  CP NMR spectrum of the same NR as A-(c). WAXD patterns B-(a) to B-(c) are obtained from the same NR as those of A-(a) to A-(c), respectively.

The  $^{13}\text{C}$  peak without the CP of the annealed NR, which is shown in Figure 3Ab, is broader than that before annealing (3Ac). The WAXD pattern presents no sharp peaks attributed to the crystalline phase. This observation suggests that there is no crystalline phase in the annealed NR. Therefore, the relatively broad peak in Figure 3Ab arises from an amorphous phase, although the  $^{13}\text{C}$  chemical shift is different. The annealing process causes random conformations of the NR chains, which result in the gauche relationship that causes a deviation in the  $\gamma$  effect. In fact, the diffraction angle of the halo peak is also shifted from  $2\theta = 19.3^\circ$  to  $18.8^\circ$ . Consequently, we conclude that the  $^{13}\text{C}$  chemical shift of the annealed NR moves slightly downfield due to the random conformation, causing the linewidth to be broader than the pristine NR without annealing.

The WAXD pattern of the maximum extended NR clearly shows a typical amorphous signal, as shown in Figure 3Ba. Furthermore, the halo peak is observed at the same position as that of the annealed NR. This observation strongly indicates that the apparent doublet peak shown in Figure 3Aa does not arise from the crystalline phase. Therefore, the doublet peak is likely caused by the existence of molecular orientation.

#### Angle-dependent $^{13}\text{C}$ NMR spectra

To investigate the molecular orientation for the maximum extended NR thin film, we measured the angle (position)-dependent  $^{13}\text{C}$  NMR spectra. We used two types of strips that were cut from a cylindrically extended, very thin NR film, as shown in Figure 1b and c. The  $0^\circ$  position is defined as the strip in a rotor set at the bottom toward the static magnetic field. The position definition is illustrated in Figure 1d and e for the  $0^\circ$  and  $90^\circ$  positions, respectively.

Figure 4a shows the angle-dependent  $^{13}\text{C}$  NMR spectra of the strip cut from the maximum extended NR shown in Figure 1b. The cutting direction is the same as the height direction of cylindrical rotor.

Figure 4a shows the sigmoidal change that depends on the sample position. Furthermore, it is clear that the  $^{13}\text{C}$  peaks of (b) to (i) are isotropic and approximately symmetric. The half widths of these peaks are between 120 and 160 Hz and are comparable to those obtained before MAS, as shown in Figure 2a (approximately 150 Hz). Furthermore, those values were less than the adamantine peak observed in the static state (ca. 250 Hz). These results suggest that the shimming was good and did not significantly affect the linewidth of the angle-dependent  $^{13}\text{C}$  NMR measurement. The  $^{13}\text{C}$  chemical shift value of (e) is the same as that shown in (i) because the angle dependence in the  $^{13}\text{C}$  NMR spectrum is the same; specifically, the dependence at the  $180^\circ$  position is the same as that at the  $0^\circ$  position. Similar criteria hold for the other spectra. For the spectra at the  $135^\circ$  (f) and  $315^\circ$  (b) positions, however, their chemical shift values do not coincide with each other. The spectrum at  $315^\circ$  (b) was finally measured after an elapsed time of  $>11$  h; therefore, the strip is slightly bent. This bending is the reason why the chemical shift at  $315^\circ$  (b) presents a different value from that at  $135^\circ$  (f).

The  $^{13}\text{C}$  peak obtained from the  $0^\circ$  position appears at 134.4 p.p.m. (i), but the peak for the  $90^\circ$  position is observed at 131.9 p.p.m. (g). The peak for the  $0^\circ$  position appears downfield to that for the  $90^\circ$  position. Similarly, the  $^{13}\text{C}$  peak for the  $45^\circ$  position appears at a middle value of 133.8 p.p.m. This tendency resembles that of the previous study except for the absolute values. Kimura *et al.*<sup>6,7</sup> investigated the relationship between the  $^{13}\text{C}$  chemical shift of vulcanized NR and the angle defined between the stretching direction of NR and the applied static magnetic field. The difference in the absolute values of the  $^{13}\text{C}$  chemical shift between our results and theirs arises from the vulcanization. Their observations indicated that for the vulcanized NR stretched perpendicular to the static magnetic field, the isotropic  $^{13}\text{C}$  peak is observed downfield to that for the NR stretched parallel to the static

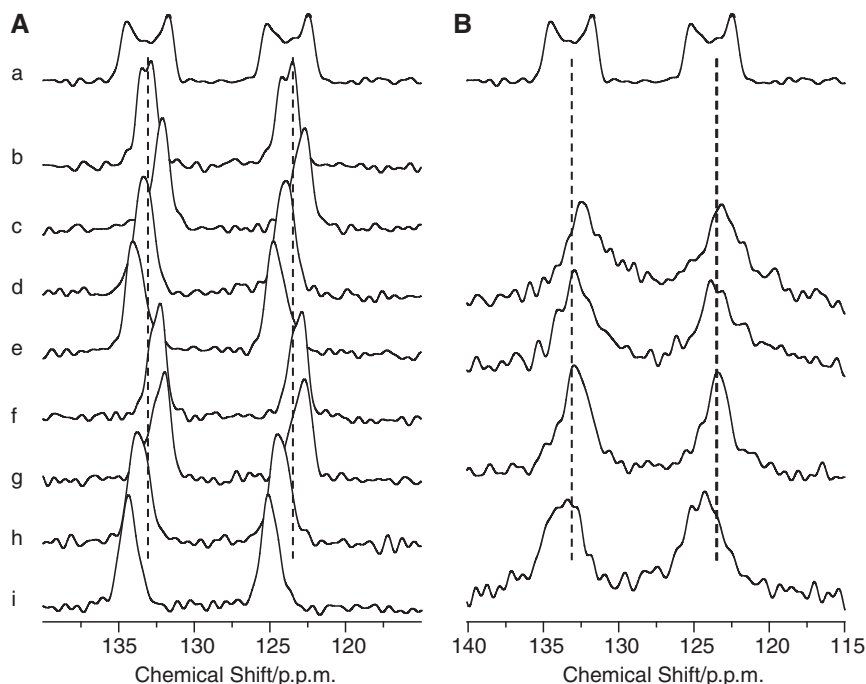


**Figure 4** Angle-dependent  $^{13}\text{C}$  NMR spectra of a strip obtained from the maximum rolled NR. **A**-(b) to (i) are obtained from the strip depicted on Figure 1b. **B**-(d), (e), (g) and (i) are observed for the strip shown in Figure 1c. The sample positions of (b) to (i) are  $315^\circ$ ,  $270^\circ$ ,  $225^\circ$ ,  $180^\circ$ ,  $135^\circ$ ,  $90^\circ$ ,  $45^\circ$  and  $0^\circ$ , respectively. Both **A**-(a) and **B**-(a) are measured from the maximum rolled NR and the same spectrum of the double-bonded region as Figure 2c. The dashed lines represent the isotropic chemical shift as shown in Figure 2a and d.

magnetic field. For the stretched NR, it is reasonable to consider that the molecular orientation of the NR chains occurs toward the stretching direction. Therefore, for the perpendicular stretching condition, the angle between the oriented NR chains and the static magnetic field is perpendicular, and for the parallel stretching condition, the NR chains are oriented parallel to the static magnetic field. In this study, the direction of the rotor has already been defined as the magic angle because of the use of a typical MAS probe. However, we can determine the molecular orientation direction by comparing our observations with those of Kimura *et al.*<sup>6,7</sup>

From the  $^{13}\text{C}$  chemical shift relationship, it is considered that the molecular orientation of the NR chains occurs toward the short side of the strip, namely the direction of the circumference and spinning of the rotor, because the  $^{13}\text{C}$  peaks observed at the  $0^\circ$  and  $90^\circ$  positions correspond to the perpendicular and the parallel stretching conditions, respectively. The angle between the short side of the NR strip and the static magnetic field becomes perpendicular, even though the rotor is at the magic angle. Although the direction of the molecular orientation is set perpendicular to the static magnetic field, the alignment of the oriented NR chains becomes the magic angle. Therefore, the shielding tensor vectors rotate by the magic angle; thus, the difference in the  $^{13}\text{C}$  chemical shifts between the  $0^\circ$  and  $90^\circ$  positions becomes smaller than the value for the circularly stretched NR observed by Kimura *et al.*<sup>6</sup> Consequently, we conclude that the NR chains are oriented toward the direction of the circumference and spinning of the rotor during MAS.

If the NR chains orient with the direction of the circumference and spinning during MAS, the  $^{13}\text{C}$  NMR spectra for the strip cut along the direction of the circumference, as shown in Figure 1c, do not show the angle dependence because the molecular orientation against the static magnetic field at the  $0^\circ$  position becomes the same as that at the  $90^\circ$  position. The molecular orientation direction becomes the

magic angle against the static magnetic field for all positions; therefore, the long side of the strip becomes the orientation direction. This invariance indicates that the observed  $^{13}\text{C}$  peaks at every angle position have the same chemical shift, which is near the isotropic value. The  $^{13}\text{C}$  NMR spectra measured at the  $0^\circ$  and  $90^\circ$  positions, at least, will suffice to confirm whether the molecular orientation occurs along the circumference direction. Figure 4b presents some of the  $^{13}\text{C}$ -angular-dependent spectra of the strip that were shown in Figure 1c. All of the  $^{13}\text{C}$  peaks appear at the same chemical shift, which is near the isotropic value. In particular, the chemical shift value of the  $0^\circ$  (i) and  $180^\circ$  (e) positions is comparable to that observed at the  $90^\circ$  position (g). This observation also suggests that the NR chains are oriented along the circumference and spinning direction during MAS.

Similarly, we also examined the NR strips at several elongation ratios. Figure 5c–g show the angle-dependent  $^{13}\text{C}$  NMR spectra of five types of NR strips at the  $0^\circ$  (dashed line) and  $90^\circ$  (solid line) positions. Figure 5a, b and h are the  $^{13}\text{C}$  spectra of the as-received annealed NR, the doughnut-shaped NR and the maximum elongated NR, respectively. Note that the  $^{13}\text{C}$  chemical shift of the strip cut from the doughnut-shaped NR is observed upfield at the  $0^\circ$  position (c), and the chemical shift value is comparable to that obtained for the maximum elongated NR at the  $90^\circ$  position (g). Furthermore, the  $^{13}\text{C}$  chemical shift of the strip cut from the doughnut-shaped NR at the  $90^\circ$  position was observed downfield. Every angle-dependent  $^{13}\text{C}$  NMR spectrum for the strip cut from the doughnut-shaped NR was completely inverse to the strip cut from the maximum elongated NR.

The  $^{13}\text{C}$  NMR peak of the quaternary carbon at the  $90^\circ$  position (solid lines) gradually shifts from 133.8 p.p.m. for the strip of the doughnut-shaped NR (c) to 132.0 p.p.m. for the maximum elongated NR (g). A similar relationship holds for the  $^{13}\text{C}$  NMR spectra at the  $0^\circ$  position (dashed lines). Therefore, it is feasible to conclude the



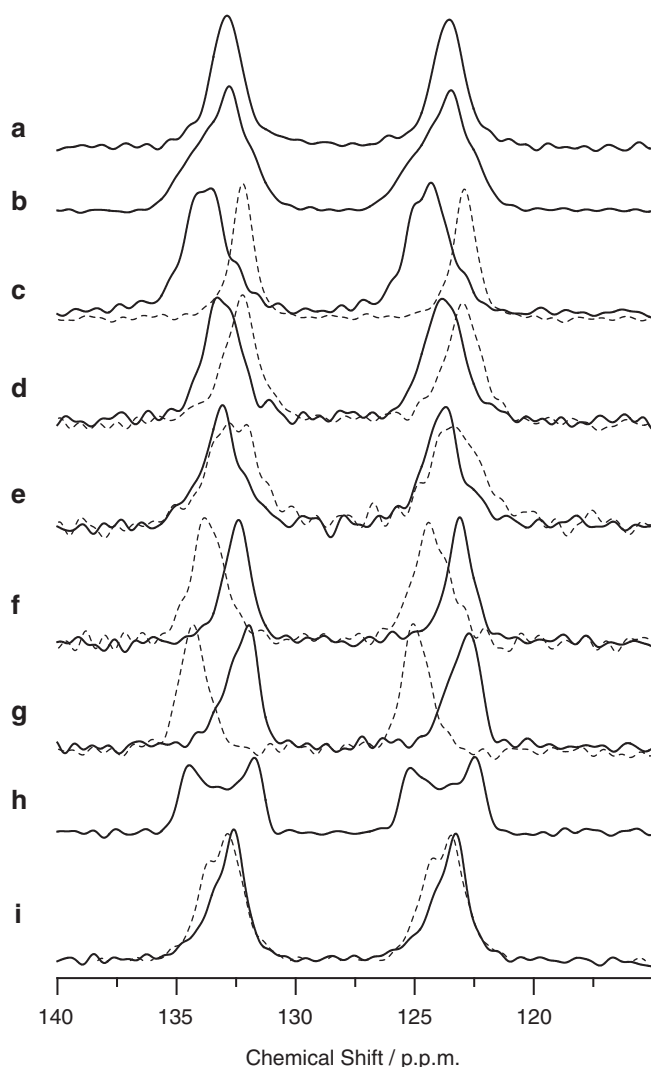


**Figure 5** Angle-dependent  $^{13}\text{C}$  NMR spectra of the strips obtained from a rolled NR with various lengths and thickness. The spectra shown in (c) to (g) and (i) are observed at the  $0^\circ$  (dashed line) and  $90^\circ$  (solid line) sample positions. Spectra (a), (b) and (h) are the same as those in Figure 2a, b and c, respectively. The length and thickness of the strips are 3.4 mm and 1.1 mm for (c), 4.4 mm and 0.8 mm for (d), 5.4 mm and 0.6 mm for (e), 8.4 mm and 0.4 mm for (f) and 20 mm and 0.2 mm for (g). The values of thickness from (d) to (g) are estimated with the assumption that each volume is the same as that of (c). Spectrum (i) is obtained from a strip that superimposed three strips of (g).

existence of a critical point where the  $^{13}\text{C}$  peaks at both the  $0^\circ$  and  $90^\circ$  positions resonate at almost the same chemical shift. The spectra at the  $0^\circ$  and  $90^\circ$  positions, which are shown in (e), are observed to be identical. These chemical shift changes can be ascribed to the diversity of the molecular orientation direction, based on the thickness during elongating by MAS. To confirm the relationship between the molecular orientation and the chemical shift, we observed the angle-dependent  $^{13}\text{C}$  NMR spectra of three superimposed strips cut from the maximum elongated NR (i). The superimposition was performed carefully so that the directions of each strip became identical to each other. The thickness becomes approximately 0.6 mm and the same value as that in (e). If the molecular orientation determines the  $^{13}\text{C}$  chemical shift, the  $^{13}\text{C}$  NMR spectrum of the superimposed strip should show the same tendency as that shown in

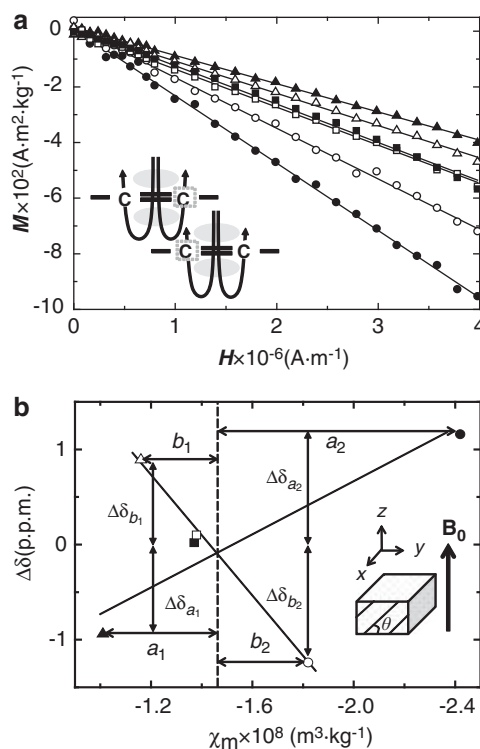


**Figure 6** (a) Observed magnetisms of strips obtained from the doughnut-shaped NR ( $\blacktriangle$  and  $\triangle$ ), the 5.4-mm-long cylindrical NR ( $\blacksquare$  and  $\square$ ) and the maximum rolled very thin film ( $\bullet$  and  $\circ$ ) of NR. The used strips are cut as shown in Figure 1b. The solid and open symbols represent the difference in the direction between an NR strip and the magnetic field  $H$ , respectively. The direction for the solid symbols corresponds to  $0^\circ$  defined in Figure 1d and for the open symbols to  $90^\circ$  shown in Figure 1e. The strips are not set at the magic angle; therefore, the strip at the  $0^\circ$  position is set perpendicular to the  $H$ . The face of the strip is perpendicular to the  $H$ . At the  $90^\circ$  position, the width (short side) of the strip is parallel to the  $H$ . The arrows of the insert represent the magnetic lines induced by  $\pi$  electrons, which are represented by gray ellipses. (b): The chemical shift difference  $\Delta\delta$  from the isotropic chemical shift value  $\delta_{\text{iso}}$  against the magnetic susceptibility  $\chi_m$ . The insert represents the effective angle between the double bond of NR and the static magnetic field  $B_0$ . The symbols are the same as those in (a).

(g) because the orientation is the same. However, Figure 5i shows that the  $^{13}\text{C}$  NMR spectral pattern for the superimposed strips at both the  $0^\circ$  and  $90^\circ$  positions exhibits almost the same tendency as in (e). This similarity suggests that the thickness is also related to the  $^{13}\text{C}$  chemical shift. Consequently, it is necessary to consider that the change in the  $^{13}\text{C}$  chemical shift that depends on the angle against the static magnetic field is not only related to the molecular orientation but also to the thickness. The thickness is presumably related to the magnetic susceptibility. The magnetic susceptibility differs depending on the direction of the double bond in NR; therefore, the  $\pi$  electrons in the double bond interact with the static magnetic field.

#### Magnetic susceptibility differences

To investigate the difference in magnetic susceptibility between the sample positions against the static magnetic field, we observed the magnetization,  $M$  ( $\text{A m}^2 \text{kg}^{-1}$ ), of the strip obtained from both the doughnut-shaped and the maximum elongated thin NR samples. In addition, the  $M$  value of the strip from the 5.4-mm-long cylindrical NR (the same sample shown in Figure 5e) was also measured.

Magnetizations in both the parallel and perpendicular directions to the magnetic field,  $H$  ( $\text{A m}^{-1}$ ), were observed. The plots of  $M$  vs  $H$  are depicted in Figure 6a. The slope represents the mass magnetic susceptibility,  $\chi_m$  ( $\text{m}^3 \text{kg}^{-1}$ ), and negative values (diamagnetic property) are generally obtained for polymers. The circles represent the strip cut from the maximum elongated NR, the triangles from the doughnut-shaped NR, and the squares from the 5.4-mm-long cylindrical NR. The solid symbols are obtained from the perpendicular direction and correspond to the  $0^\circ$  position; the open symbols represent the parallel directions that correspond to the  $90^\circ$  position. Figure 6a indicates that the slope of the strip cut from the maximum elongated NR is considerably steeper than those cut from the doughnut and cylindrical NRs. Furthermore, it is also clear that the slope for the perpendicular direction is different from that for the parallel, especially for the strip cut from the maximum elongated NR.

For the strip cut from the maximum elongated NR, the negative slope for the perpendicular direction ( $\bullet$ ,  $-2.42 \times 10^{-8} \text{m}^3 \text{kg}^{-1}$ ) is greater than that for the parallel direction ( $\circ$ ,  $-1.82 \times 10^{-8} \text{m}^3 \text{kg}^{-1}$ ). This observation indicates that the diamagnetism for the perpendicular direction is greater than that for the parallel direction and indicates that the double bonds are regularly aligned along the molecular orientation direction. The chemical shifts of double-bonded carbons generally move downfield because of the paramagnetic effect from the  $\pi$  electrons compared with the aliphatic carbons. However, the overall apparent diamagnetism of the molecules increases because of the regularly aligned  $\pi$  electron clouds. The  $\pi$  electron clouds in the aligned double bonds induce a paramagnetic effect on the intermolecular chains, as illustrated in the insert of Figure 6a. Thus, the decrease of the magnetic susceptibility, that is, the increase of the absolute value (slope), for the perpendicular direction suggests the downfield shift of the  $^{13}\text{C}$  NMR peaks. Therefore, the magnetic susceptibility results are in agreement with the  $^{13}\text{C}$  NMR observation: the  $^{13}\text{C}$  NMR peak at the  $0^\circ$  position was observed downfield to that at the  $90^\circ$  position for the maximum elongated NR (Figure 4a).

In contrast, for the strip cut from the doughnut-shaped NR, the slope for the perpendicular direction ( $-1.01 \times 10^{-8} \text{m}^3 \text{kg}^{-1}$ ) is slightly gradual compared with that for the parallel direction ( $-1.16 \times 10^{-8} \text{m}^3 \text{kg}^{-1}$ ). The relationship for the strip cut from the doughnut-shaped NR becomes inverse to the relationship for the strip cut from the maximum elongated NR. This inverse relationship is in agreement with the  $^{13}\text{C}$  NMR observations shown in Figure 5, although the chemical shift difference between the  $0^\circ$  and  $90^\circ$  positions for the doughnut-shaped NR was not small; however, it was comparable to that obtained from the maximum elongated NR.

Note that for the 5.4-mm-long cylindrical NR, the slope for the perpendicular direction ( $-1.37 \times 10^{-8} \text{m}^3 \text{kg}^{-1}$ ) was equivalent to that for the parallel direction ( $-1.38 \times 10^{-8} \text{m}^3 \text{kg}^{-1}$ ). This observation is in agreement with the observation that the chemical shift for the  $0^\circ$  position is the same as that for the  $90^\circ$  position, as shown in Figure 5e.

Figure 6a suggests that the magnetic susceptibility strength changes depending on the angle between the direction of the strip and the static magnetic field and the thickness of the strip. The NR  $^{13}\text{C}$  chemical shift is attributed to the interaction between the applied static magnetic field and the magnetic susceptibility. For the maximum elongated NR, because the high inner pressure caused by MAS results in the NR chains to roll out and orient, almost all of the NR chains regularly align along the same circumference direction during MAS. For the doughnut-shaped NR, however, the inner pressure is limited because the radius from the center of the rotor to the surface of the NR is small. The oriented NR chains in the

doughnut-shaped NR are, presumably, slightly oblique from the circumference direction.

The above consideration and results imply that the observed chemical shift is estimated from the magnetic susceptibility. To clarify the relationship between the chemical shift observed for the angle-dependent  $^{13}\text{C}$  NMR spectra and the magnetic susceptibility,  $\chi_m$ , we plotted the chemical shift difference,  $\Delta\delta$ , from the isotropic chemical shift value,  $\delta_{\text{iso}}$ , vs the  $\chi_m$  value:  $\Delta\delta = \delta_{\text{iso}} - \delta$  at the  $0^\circ$  or  $90^\circ$  position. Figure 6b presents the relationship between  $\Delta\delta$  and  $\chi_m$  for both the perpendicular and parallel directions of the maximum elongated, the doughnut-shaped and the 5.4-mm-long cylindrical NR. The symbols are the same as shown in Figure 6a. Figure 6b indicates that the change in the  $\chi_m$  values from the doughnut-shaped NR to the maximum elongated NR at both the perpendicular and parallel directions is proportional to the chemical shift change (solid lines are obtained from the least-squares fit). The point of the intersection (dashed line) indicates that the contribution of the magnetic susceptibility to the chemical shift becomes negligible, namely that the  $\chi_m$  value at the point ( $\chi_m^0$ ) corresponds to the isotropic chemical shift. This observation supports the idea that the  $\chi_m$  values for the strip obtained from the 5.4-mm-long cylindrical NR ( $\blacksquare$  and  $\square$ ) are very close to  $\chi_m^0$ .

We assumed that the magnetic susceptibility difference is proportional to the chemical shift difference, and its absolute value arises from the degree of strain (thickness). Furthermore, we defined the effective angle,  $\theta_i$ , between the direction of the NR double bond and the applied static magnetic field:  $i$  assumes values of 1 or 2 for the doughnut-shaped or the maximum elongated NR in the sample rotor, respectively. The effective angle is not the real angle of the molecular orientation, but it affects the observed chemical shift. Because the  $z$ -axis component of the magnetic susceptibility (direction of the magnetic field) contributes to the observed chemical shift, the value of  $|\chi_m^0 - \chi_m| \cos(90^\circ - \theta_i)$  at the perpendicular direction (corresponding to the  $0^\circ$  position) is proportional to the absolute value of  $\Delta\delta$ . Therefore, the two equations for the doughnut-shaped NR can be stated as follows:

$$k_1 \cdot a_1 \cdot \cos(90^\circ - \theta_1) = \Delta\delta_{a1} \quad (1)$$

$$k_1 \cdot b_1 \cdot \sin(90^\circ - \theta_1) = \Delta\delta_{b1} \quad (2)$$

where  $k_1$  is the proportional constant and expresses the chemical shift value per the unit magnetic susceptibility for the doughnut-shaped NR. The values of  $a_1$  and  $b_1$  are the magnetic susceptibility difference  $|\chi_m^0 - \chi_m|$  at the perpendicular and the parallel directions for the doughnut-shaped NR.  $\Delta\delta_{a1}$  and  $\Delta\delta_{b1}$  are the corresponding chemical shifts for  $a_1$  and  $b_1$ , respectively. Similar equations are also derived for the maximum elongated NR. From both Equations (1) and (2), we estimated the  $k_1$  and  $\theta_1$  values to be approximately  $3.6 \text{ p.p.m. m}^{-3} \text{ kg}^{-1}$  and  $35^\circ$ , respectively. Similarly,  $k_2$  and  $\theta_2$  are estimated to be approximately  $3.6 \text{ p.p.m. m}^{-3} \text{ kg}^{-1}$  and  $19^\circ$  for the maximum elongated NR, respectively. The values of  $k_1$  and  $k_2$  were identical, indicating that the equations are reasonable because the contribution from the unit magnetic susceptibility to the chemical shift should be the same. The obtained effective angle of the doughnut-shaped NR is larger than that obtained for the maximum elongated NR. This difference suggests that the alignment of the NR chains is slightly oblique to the circumference direction. Furthermore, the chemical shift value per the unit magnetic susceptibility of  $3.6 \text{ p.p.m. m}^{-3} \text{ kg}^{-1}$  indicates that the  $\Delta\delta$  between perpendicular and parallel positions observed using the static probe becomes

3.6 p.p.m. This value is in excellent agreement with the chemical shift anisotropy (3.5–3.7 p.p.m.) estimated by Kimura *et al.*<sup>6</sup>

Consequently, we conclude that the reason why the angle-dependent  $^{13}\text{C}$  NMR spectra obtained from the strip of the doughnut-shaped NR become reversed compared with the strip from the maximum elongated NR is due to both the magnetic susceptibility difference and the chain orientation. As stated above, the magnetic susceptibility of the well-ordered NR chains in the maximum elongated NR is very sensitive to its angle against the static magnetic field; therefore, almost all of the  $\pi$  electron clouds regularly align. This regularity causes the  $^{13}\text{C}$  chemical shift to distinctly change depending on the position of the strip against the static magnetic field, which results in the apparent doublet peak. In contrast, the  $^{13}\text{C}$  chemical shift difference between the  $0^\circ$  and  $90^\circ$  positions for the strip cut from the doughnut-shaped NR is comparable to that from the maximum elongated NR; however, the magnetic susceptibility difference between the perpendicular and the parallel directions for the strip cut from the doughnut-shaped NR is considerably smaller than that from the maximum elongated NR because the alignment of the NR chains is slightly oblique.

## CONCLUSIONS

We presented the static  $^{13}\text{C}$  NMR spectra of NR that was deformed during MAS. The molecular-oriented strain induces the  $^{13}\text{C}$  chemical shift change of NR. WAXD did not show the existence of crystalline phase for the maximum elongated NR. The angle-dependent  $^{13}\text{C}$  NMR spectra of NR of several thicknesses indicated that the strain-induced  $^{13}\text{C}$  chemical shift change depends not only on the molecular orientation but also on the magnetic susceptibility.

## ACKNOWLEDGEMENTS

We are grateful to S Kawahara, Y Nishitani, N Kuramoto, T Saito, T Kitai, N Watanabe, N Kitagawa, T Iwai, Y Tominaga, H Hirahara, H Yamamoto and K Takenaka, members of the Advanced Elastomer research group in the Society of Rubber Industry, Japan, for their kind discussion and cooperation in completing this study. We also thank Dr DL VanderHart of the National Institute of Standards and Technology for his helpful advice regarding the magnetic susceptibility measurements.

- 1 Kawahara, S., Chaikumpollert, O., Sakurai, S., Yamamoto, Y. & Akabori, K. Crosslinking junctions of vulcanized natural rubber analyzed by solid-state NMR spectroscopy equipped with field-gradient-magic angle spinning probe. *Polymer* **50**, 1626–1631 (2009).
- 2 Asano, A., Hori, S., Kitamura, M., Nakazawa, C. T. & Kurotsu, T. Influence of magic angle spinning on  $T_1^H$  of SBR studied by solid state  $^1\text{H}$  NMR. *Polym. J.* (e-pub ahead of print 7 March 2012; doi:10.1038/pj2012.10).
- 3 Kawamura, I., Degawa, Y., Yamaguchi, S., Nishimura, K., Tuzi, S., Saito, H. & Naito, A. Pressure-induced isomerization of retinal on bacteriorhodopsin as disclosed by fast magic angle spinning NMR. *Photochem. Photobiol.* **83**, 346–350 (2007).
- 4 Nishiyama, Y., Frey, M. H., Mukasa, S. & Utsumi, H.  $^{13}\text{C}$  solid-state NMR chromatography by magic angle spinning  $^1\text{H}$   $T_1$  relaxation ordered spectroscopy. *J. Magn. Reson.* **202**, 135–139 (2010).
- 5 Fry, E. A., Sengupta, S., Phan, V. C., Kuang, S. & Zilm, K. W. CSA-Enabled spin diffusion leads to MAS Rate-Dependent  $T_1$ 's at High Field. *J. Am. Chem. Soc.* **133**, 1156–1158 (2011).
- 6 Kimura, H., Dohi, H., Kotani, M., Matsunaga, T., Yamauchi, K., Kaji, H., Kurosu, H. & Asakura, T. Molecular dynamics and orientation of stretched rubber by solid-state  $^{13}\text{C}$  NMR. *Polym. J.* **42**, 25–30 (2010).
- 7 Dohi, H., Kimura, H., Kotani, M., Matsunaga, T., Yamauchi, K., Kaji, H. & Asakura, T. Characterization of molecular orientation of stretched natural rubber by solid-State  $^{13}\text{C}$  NMR. *Polym. J.* **39**, 502–503 (2007).
- 8 Lin, W., Bian, M., Yang, G. & Chen, Q. Strain-induced crystallization of natural rubber as studied by high-resolution solid-state  $^{13}\text{C}$  NMR spectroscopy. *Polymer* **45**, 4939–4943 (2004).